Biochimica et Biophysica Acta 1840 (2014) 2321–2330

Contents lists available at ScienceDirect

Biochimica et Biophysica Acta

journal homepage: www.elsevier.com/locate/bbagen

Neuroprotective effect of PEP-1-peroxiredoxin2 on CA1 regions in the hippocampus against ischemic insult

Hoon Jae Jeong [a,1], Dae Young Yoo [b,1], Dae Won Kim [c,1], Hyeon Ji Yeo [a], Su Bin Cho [a], Jiye Hyeon [a], Jung Hwan Park [a], Jinseu Park [a], Won Sik Eum [a], Hyun Sook Hwang [a], Moo-Ho Won [d], In Koo Hwang [b,*], Soo Young Choi [a,**]

[a] Department of Biomedical Sciences, Research Institute of Bioscience and Biotechnology, Hallym University, Chunchon 200-702, Republic of Korea
[b] Department of Anatomy and Cell Biology, College of Veterinary Medicine, Research Institute for Veterinary Science, Seoul National University, Seoul 151-742, Republic of Korea
[c] Department of Biochemistry and Molecular Biology, Research Institute of Oral Sciences, College of Dentistry, Kangnung–Wonju National University, Gangneung 210-702, Republic of Korea
[d] Department of Neurobiology, School of Medicine, Kangwon National University, Chuncheon 200-701, Republic of Korea

ARTICLE INFO

Article history:
Received 8 July 2013
Received in revised form 1 March 2014
Accepted 4 March 2014
Available online 12 March 2014

Keywords:
Peroxiredoxin2
Ischemic insult
Oxidative stress
Protein transduction domain
Apoptosis pathway

ABSTRACT

Background: Oxidative stress is a leading cause of various diseases, including ischemia and inflammation. Peroxiredoxin2 (PRX2) is one of six mammalian isoenzymes (PRX1–6) that can reduce hydrogen peroxide (H_2O_2) and organic hydroperoxides to water and alcohols.
Methods: We produced PEP-1-PRX2 transduction domain (PTD)-fused protein and investigated the effect of PEP-1-PRX2 on oxidative stress-induced neuronal cell death by 3-(4,5-dimethylthiazol-2-yl)-2,5-diphenyltetrazolium bromide (MTT) assay, Western blot, immunofluorescence microscopy, and immunohistochemical analysis.
Results: Our data showed that PEP-1-PRX2, which can effectively transduce into various types of cells and brain tissues, could be implicated in suppressing generation of reactive oxygen species, preventing depolarization of the mitochondrial membrane, and inhibiting the apoptosis pathway in H_2O_2-stimulated HT22, murine hippocampal neuronal cells, likely resulting in protection of HT22 cells against H_2O_2-induced toxicity. In addition, we found that in a transient forebrain ischemia model, PEP-1-PRX2 inhibited the activation of astrocytes and microglia in the CA1 region of the hippocampus and lipid peroxidation and also prevented neuronal cell death against ischemic damage.
Conclusions: These findings suggest that the transduced PEP-1-PRX2 has neuroprotective functions against oxidative stress-induced cell death *in vitro* and *in vivo*.
General significance: PEP-1-PRX2 could be a potential therapeutic agent for oxidative stress-induced brain diseases such as ischemia.

1. Introduction

Oxidative stress is due to the overproduction of reactive oxygen species (ROS) and other radicals. Abnormally increased ROS damage cells by altering cellular components, including proteins, fatty acids, and DNA [1]. Ischemia/reperfusion injury is the pathological condition caused when blood supply to an area of tissue, including the brain, is returned after being interrupted. In ischemia/reperfusion, ROS, produced in excess quantities, could result in neuronal cell death in the CA1 region of the hippocampus [2].

Peroxiredoxin1–6 (PRX1–6) act as an antioxidant by converting various peroxides, including H_2O_2 and various organic hydroperoxides, into water and alcohols using the electrons that thioredoxin donates, except for PRX6 that utilizes glutathione instead of thioredoxin [3]. Together with modulating ROS concentration, PRXs have various cellular functions. For example, PRX2 appears to modulate growth factors and the tumor necrosis factor-alpha-mediated signaling pathway *via* modulating endogenous H_2O_2 signaling [4]. Also, it has been suggested that PRXs are associated with cellular differentiation, such as vascular remodeling [5,6]. In response to pathogens and external stresses, PRXs function as a chaperone [7]. Therefore, increased expression of PRXs in the neurons could attenuate neuronal cell injury caused by ROS production, leading to prevention of ischemia and reperfusion in the brain.

In this study, we investigated whether PEP-1-PRX2 could protect HT22 murine hippocampal neuronal cells against H_2O_2-induced cell death and the hippocampal CA1 regions against the transient forebrain ischemia in a gerbil model. We demonstrated that PEP-1-PRX2

* Corresponding author. Tel.:+82 33 248 2112; fax: +82 33 241 1463.
** Correspondence to: S.Y. Choi, Department of Biomedical Science, Research Institute of Bioscience and Biotechnology, Hallym University, Chunchon 200-702, Republic of Korea. Tel.: +82 33 248 2112; fax: +82 33 241 1463.
E-mail addresses: vetmed2@snu.ac.kr (I.K. Hwang), sychoi@hallym.ac.kr (S.Y. Choi).
[1] These authors contributed equally to this work.

http://dx.doi.org/10.1016/j.bbagen.2014.03.003
0304-4165/

efficiently transduced into neuronal cells in the brain and that PEP-1-PRX2 may be a potential therapeutic agent for transient forebrain ischemia.

2. Material and methods

2.1. Cells and materials

HT22, murine hippocampal neuronal cells, were cultured in DMEM supplemented with 10% fetal bovine serum (FBS) and antibiotics at 37 °C under humidified conditions of 95% air and 5% CO_2. PEP-1 peptide was chemically synthesized from Peptron (Daejeon, Korea). All other chemicals and reagents were of the highest commercial grade available.

2.2. Transduction of PEP-1-PRX2 into HT22 cells

PRX2 and PEP-1-PRX2 proteins were prepared as described previously [8]. Protein samples were collected from the processes of purifying PEP-1-PRX2 and PRX2 and the purity of the samples was assessed using SDS-PAGE and Western blot analysis. All protein samples were prepared in a buffer containing a reducing agent and dithiothreitol (DTT) to only show a monomer of PEP-1-PRX2 or PRX2.

To confirm whether PEP-1-PRX2 undergoes monomer–dimer shift as PRX2 does, purified PEP-1-PRX2 was prepared in a buffer with or without DTT. Also, to examine whether a disulfide bond between two subunits of PEP-1-PRX2 could form in the process of catalysis of H_2O_2, a substrate of PRX2, a monomer of PEP-1-PRX2 containing DTT was exposed to H_2O_2 (200 μM), subsequently leading to a dimer of PEP-1-PRX2.

To assess the dose- and time-dependent transduction of PRX2 and PEP-1-PRX2, HT22 cells were treated with various concentrations of PRX2 and PEP-1-PRX2 for 1 h or treated with PRX2 and PEP-1-PRX2 for various times. To remove proteins attached to the cellular membranes, cells were then treated with trypsin-EDTA for 10 min and washed with phosphate-buffered saline (PBS) three times. The cells were lysed with ice-cold RIPA buffer (Thermo Scientific, IL, USA) and the lysates were centrifuged at 13,000 ×*g* for 20 min at 4 °C. Protein concentration of the supernatant was quantified by the Bradford method. Equal amounts of protein were loaded into the wells of SDS-PAGE and Western blot analysis was performed using rabbit anti-His (1:2000, Santa Cruz Biotechnology) and goat anti-rabbit (1:5000, Santa Cruz Biotechnology) secondary antibodies.

Also, to assess the distributions of PRX2 and PEP-1-PRX2 in cells, HT22 cells, treated with PRX2 and PEP-1-PRX2, were probed with rabbit anti-His antibody and Alexa fluor 488 conjugated goat anti-rabbit secondary antibody (1:15,000, Invitrogen, Carlsbad, CA) and analyzed by fluorescence microscopy (Nikon eclipse 80i, Japan).

2.3. Measurement of cell viability and intracellular ROS level

To investigate cell viability, a 3-(4,5-dimethylthiazol-2-yl)-2,5-diphenyltetrazolium bromide (MTT) assay was performed as described in a previous study [9]. Intracellular ROS levels were determined using 2′,7′-dichlorofluorescein diacetate (DCF-DA), which is converted into fluorescent 2′,7′-dichlorofluorescein (DCF) by ROS [10]. Briefly, HT22 cells were incubated with PEP-1, PRX2, and PEP-1-PRX2 for 1 h and sequentially exposed to H_2O_2 (200 μM) for 30 min. After treatment with DCF-DA (20 μM), the level of DCF in the samples was measured using an ELISA plate reader (Labsystems Oy, Helsinki, Finland).

2.4. Terminal deoxynucleotidyl transferase (TdT)-mediated biotinylated dUTP nick end labeling (TUNEL) assay

TUNEL staining was performed using a Cell Death Detection kit (Roche Applied Science) according to the manufacturer's instructions. Images were taken using a fluorescence microscope.

2.5. Measurement of mitochondrial membrane potential (MMP)

The MMP was measured using a 5,5′,6,6′-tetrachloro-1,1′,3,3′-tetraethyl-benzimidazoly-carbocyanine iodine (JC-1) assay kit (Cayman, MI, USA) according to the manufacturer's instructions. JC-1 in healthy cells with high MMP forms potential-dependent JC-1-aggregates with red fluorescence in mitochondria, while mitochondrial depolarization turns JC-1 aggregates into monomers with green fluorescence [11]. HT22 cells were treated with PEP-1-PRX2 and H_2O_2. JC-1 staining solution was added to the cells (50 μl/each well of 12-well plate) at 37 °C for 15 min. JC-1 J-aggregates and JC-1 monomers in the cells were analyzed using a fluorescent microscope (Nikon eclipse 80i, Japan).

2.6. Experimental animals and induction of cerebral forebrain ischemia

Male Mongolian gerbils were maintained under standard animal care conditions. All experimental procedures involving animals and their care conformed to the Guide for the Care and Use of Laboratory Animals of the National Veterinary Research & Quarantine Service of Korea and were approved by the Hallym Medical Center Institutional Animal Care and Use Committee. Cerebral forebrain ischemia damage was induced as previously described [12]. For the histological analysis, sectioned brains were incubated with diluted mouse anti-neuronal nuclei (NeuN, 1:1000, Chemicon International, Temecula, CA), rabbit anti-glial fibrillary acidic protein (GFAP, 1:1000, Chemicon), and rabbit anti-ionized calcium-binding adapter molecule 1 (Iba-1, 1:500, Wako, Osaka, Japan) for 48 h at 4 °C. Thereafter, they were exposed to biotinylated rabbit anti-goat IgG (1:200, Vector Laboratories, Burlingame, CA) or goat anti-mouse IgG and streptavidin–peroxidase complex and visualized with 3,3′-diaminobenzidine tetrahydrochloride (Sigma-Aldrich, St. Louis, MO).

To examine the effect of PEP-1-PRX2 on spontaneous motor activity and lipid peroxidation in brains, PEP-1, PRX2, and PEP-1-PRX2 (3.0 mg/kg, n = 14/group) were administered intraperitoneally (i.p.) 30 min prior to ischemic surgery. The spontaneous motor activity was measured as previously described [12]. The spontaneous motor activity of gerbils was monitored with a Photobeam Activity System for 24 h. Each animal was observed continuously *via* a 4 × 8 photobeam. Scores were generated from live observations, and video sequences were used for subsequent re-analysis. Also, the levels of 4-hydroxy-2-nonenal (HNE) in hippocampal homogenates were measured [12].

2.7. Statistical analysis

The data presented represent the means ± SD from three independent experiments. The differences among the means were statistically analyzed by Student's *t* test. Values of $P < 0.05$, $P < 0.01$, or $P < 0.001$ were considered statistically significant.

3. Results

3.1. Expression and purification of PEP-1-PRX2

We constructed the overexpression vectors for PEP-1-PRX2, a cell permeable PRX2 protein, and PRX2, a control protein, as previously described [8]. The schematic structures of PEP-1-PRX2 and PRX2 are shown in Fig. 1A. Purified PEP-1-PRX2 and PRX2 were confirmed by Western blot analysis using an anti-His antibody (Fig. 1B and C). Because of exposure to DTT, only the monomer of PEP-1-PRX2 was found in Fig. 1B and C.

PRX2 has a high reactivity for H_2O_2 (Km ~ 0.7 μM) and an active Cys on one PRX2 subunit forms a disulfide bond with the other subunit in the presence of H_2O_2. Consequently dimeric PRX2 proteins accumulate [13]. We examined whether PEP-1-PRX2 could undergo dimerization during catalysis of H_2O_2. As shown in Fig. 1D and E, there were two

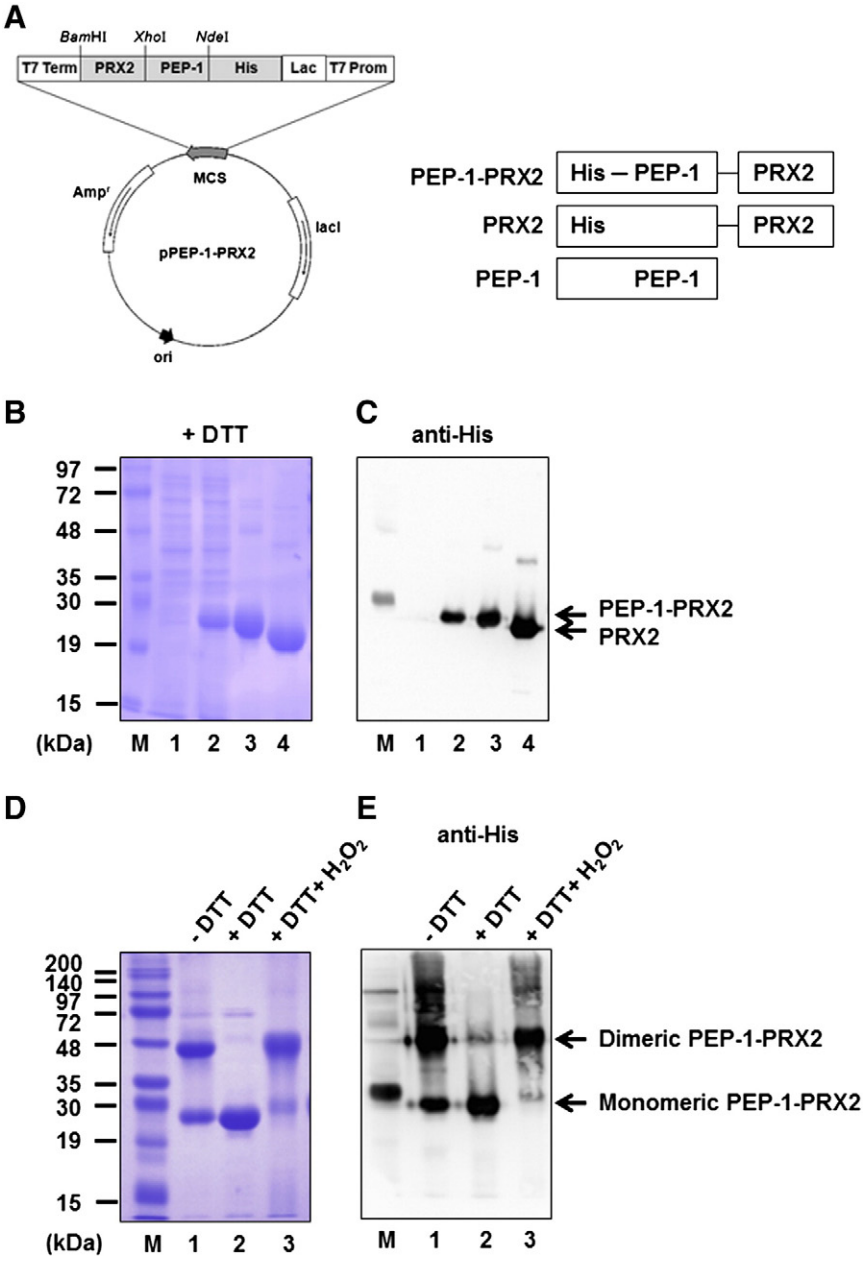

Fig. 1. Purification of PEP-PRX2 and PRX2. (A) A PEP-1-PRX2 expression vector was constructed using pET-15b. Schematic sequence of PEP-1-PRX2, PRX2, and PEP-1. His was used for the purification and detection of PEP-1-PRX2 and PRX2. (B) PEP-1-PRX2 and PRX2 proteins under the reducing condition. All protein samples containing a reducing agent, DTT, were subjected to 12% SDS-PAGE. (C) Western blot analysis shows monomers of PEP-1-PRX2 and PRX2. (B), (C) Lane M, marker (EBM-1035, Elpisbiotech, Korea); lane 1, PEP-1-PRX2 expression before induction; lane 2, PEP-1-PRX2 expression after IPTG induction; lane 3, purified PEP-1-PRX2; lane 4, purified PRX2. (D), (E) Monomer–dimer shift of PEP-1-PRX2. Monomer (~28 kDa) and dimer (~45 kDa) of PEP-1-PRX2 were identified by (D) SDS-PAGE and (E) Western blot analysis. Lane M, marker; lane 1, purified PEP-1-PRX2 without a reducing agent (DTT, 0 mM); lane 2, purified PEP-1-PRX2 in the presence of DTT (5 mM); lane 3, purified PEP-1-PRX2 in the presence of DTT (5 mM) and H_2O_2 (200 μM).

bands indicating a monomer (approximately 28 kDa) and a dimer (approximately 45 kDa) of PEP-1-PRX2 (lane 1). However, only the monomeric form of PEP-1-PRX2 (lane 2) was detected in the presence of DTT, which reduces disulfide bonds. In addition, when H_2O_2 was added to the monomeric form of PEP-1-PRX2, monomeric PEP-1-PRX2 was significantly converted to dimeric PEP-1-PRX2 (lane 3). Therefore, these results show that PEP-1-PRX2 could form the dimers during the reduction process of H_2O_2.

3.2. Transduction of PEP-1-PRX2 into HT22 hippocampal neuronal cells

We investigated whether PEP-1-PRX2 protein could transduce into HT22 cells. HT22 cells were exposed to various concentrations (0.5–3.0 μM) of PEP-1-PRX2 for 1 h or to PEP-1-PRX2 (1.0 μM) for various incubation times (30–120 min), after which levels of transduced proteins were analyzed by Western blot using an anti-His antibody. The transduced level of PEP-1-PRX2 gradually increased in a concentration- and a time-dependent manner (Fig. 2A and B). Also, consistent with the above Western blot data, our fluorescence microscopy data showed that only PEP-1-PRX2 was significantly transduced into HT22 cells (Fig. 2C). By contrast, PRX2 has no ability to transduce into cells (Fig. 2A–C). Next, the intracellular stability of PEP-1-PRX2 was examined. A considerable amount of transduced PEP-1-PRX2 was significantly detected in HT22 cells up to 24 h after exposure to PEP-1-PRX2 (Fig. 2D). According to a previous study, a protein could penetrate to target cells by either a fusion with PTDs or simply mixing with a protein and PTDs [14]. We compared the transduction efficiency of fusion and mixing methods. Our data showed that the mixing

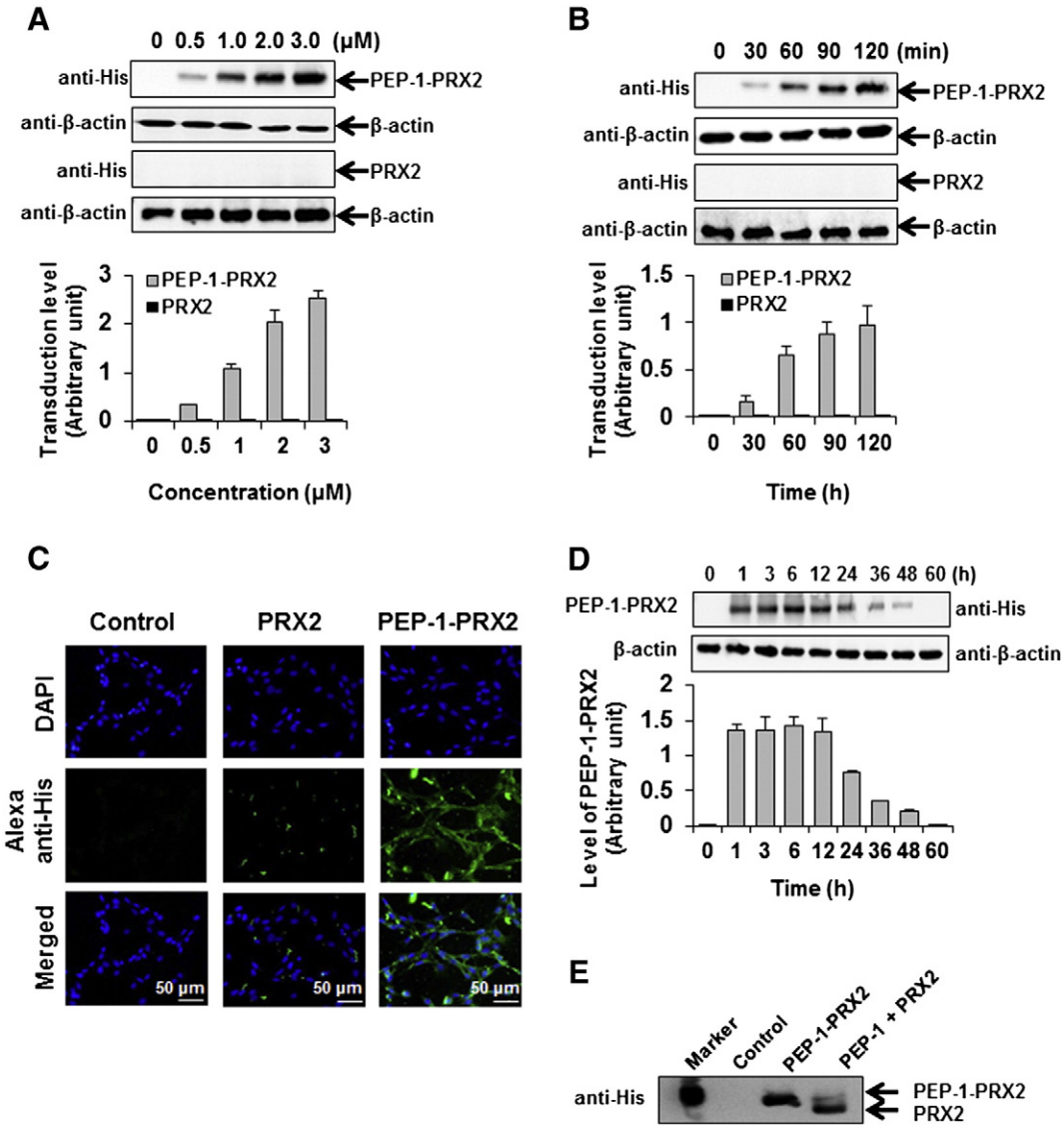

Fig. 2. Transduction of PEP-1-PRX2 into HT22 cells. To investigate (A) the dose-dependency and (B) time-dependency of transduction of PEP-1-PRX2 and PRX2, HT22 cells were treated (A) with various concentrations (0.5–3.0 μM) of PEP-1-PRX2 and PRX2 for 1 h or (B) with each protein (1.0 μM) for various incubation times (30–120 min). (C) Cellular localization of transduced PEP-1-PRX2 was analyzed using confocal fluorescence microscopy. (D) Intracellular stability of transduced PEP-1-PRX2 for 60 h. Cells were incubated with PEP-1-PRX2 (1.0 μM) for 1 h and then harvested at desired times. Arbitrary unit, a ratio of PEP-1-PRX2 or PRX2 to β-actin. (E) *In vitro* transduction efficiency of PEP-1-PRX2 and PEP-1 + PRX2 into HT22 cells. To compare the efficiency of mixing and fusion methods, HT22 cells were incubated with PEP-1-PRX2 (1 μM) or PRX2 (1 μM) + PEP-1 (20 μM) for 1 h. The amounts of PEP-1-PRX2 and PRX2 + PEP-1 to be transduced into the cells were measured by Western blot analysis.

method was as effective for the cellular transduction of PRX2 as the fusion method (Fig. 2E). These results suggest that PEP-1-PRX2 has the ability to effectively traverse the cellular membrane of HT22 cells with a half-life of less than 24 h.

3.3. Effect of PEP-1-PRX2 on H_2O_2-induced ROS production and cell viability

To investigate whether PEP-1-PRX2 protects HT22 cells under oxidative stress, cellular toxicity was induced by H_2O_2 (200 μM) for 16 h and monitored using an MTT assay. PEP-1-PRX2 (3 μM) decreased H_2O_2-induced toxicity by about 33% compared to the PRX2- and PEP-1-treated samples (Fig. 3A). To further examine the inhibitory effect of PEP-1-PRX2 on H_2O_2-induced ROS generation, ROS levels in each sample were measured 30 min after treatment with H_2O_2 (200 μM). As shown in Fig. 3B and C, the increased ROS level caused by H_2O_2 was significantly suppressed by PEP-1-PRX2. The ROS levels in the PEP-1 and PRX2 samples were similar to that in the H_2O_2-treated sample. Thus, these results demonstrate that PEP-1-PRX2 suppresses H_2O_2-induced ROS generation in HT22 cells and decreases H_2O_2-induced toxicity.

3.4. Effect of PEP-1-PRX2 on Akt activation and intrinsic apoptotic pathway induced by H_2O_2

We examined the effect of PEP-1-PRX2 on oxidative stress-induced phosphorylation of a survival signaling kinase, Akt, as well as a major cellular stress responsive protein, JNK. The phosphorylation of Akt and JNK was temporally induced 15 min post-treatment with H_2O_2. PEP-1-PRX2 suppressed H_2O_2-induced phosphorylation of Akt and JNK in a dose dependent manner, whereas PRX2 did not cause any significant reduction in the activated levels of Akt and JNK (Fig. 4A).

H_2O_2-induced neuronal cell death is mediated *via* the intrinsic apoptotic pathway, characterized by the permeabilization of the mitochondria, the release of cytochrome c from mitochondria, and finally the activation of the caspase cascade. Thus, mitochondria are a transducer of apoptotic signals in neurons. ROS induce the release of

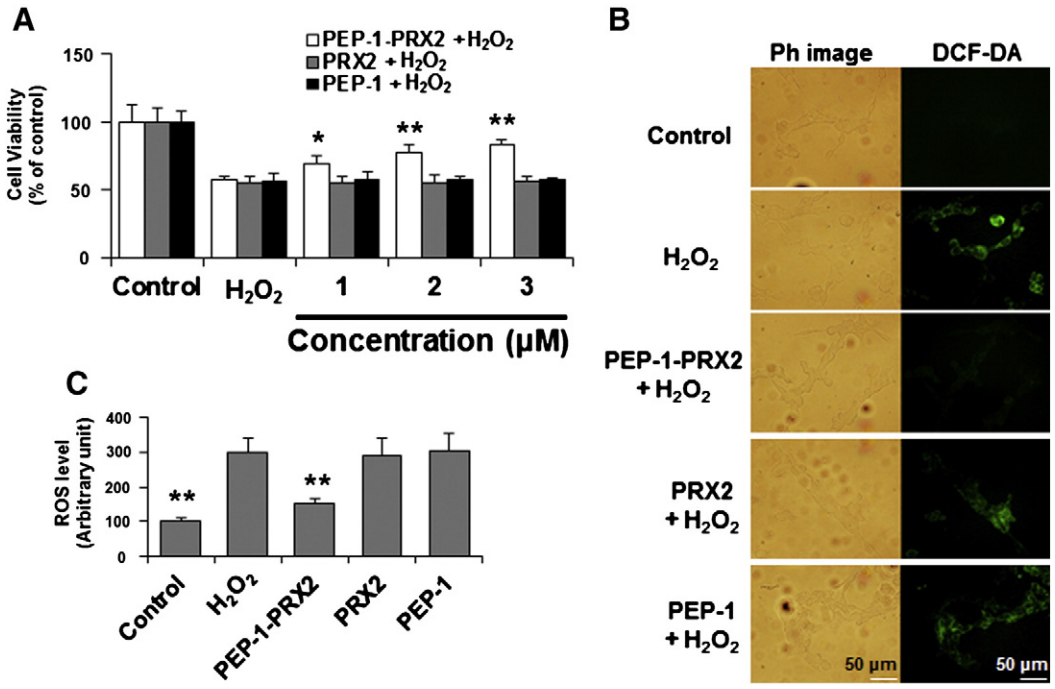

Fig. 3. PEP-1-PRX2 inhibits H_2O_2-induced ROS generation and cellular toxicity in HT22 cells. (A) HT22 cells were pretreated with PEP-1-PRX2 and PRX2 (1.0–3.0 μM) for 1 h, washed with PBS, and then exposed to H_2O_2 (200 μM) for 16 h. Cellular toxicity was evaluated using a MTT assay. (B) Suppression of H_2O_2-induced ROS generation by PEP-1-PRX2. HT22 cells were incubated with PEP-1, PRX2, and PEP-1-PRX2 (3.0 μM) for 1 h, washed with PBS, and then treated with H_2O_2 (200 μM) for 30 min. Following incubation, the cells were stained with DCF-DA. Ph image, phase contrast image. (C) Measurement of ROS level. The bar graph represents means ± SD from three independent experiments. Data was analyzed by Student's *t* test. $^*P < 0.05$ and $^{**}P < 0.001$ between H_2O_2 and other groups.

cytochrome c from the mitochondrial membrane *via* phosphorylation of p53, an important regulator of apoptosis, by MAPK and the expression of several genes, including Bax and Bid, by phosphorylated p53 [1]. First, Fig. 4B shows that PEP-1-PRX2 significantly inhibited the phosphorylation of p53, compared with PRX2. Apoptotic signals often converge on the mitochondria, leading to a change in the permeability of the outer mitochondrial membrane and a decrease in the MMP. We measured whether PEP-1-PRX2 relieves H_2O_2-induced disruption of the MMP using JC-1, a fluorescent mitochondrial-specific cationic dye. H_2O_2 treatment showed the bright green fluorescence, indicating the disturbed MMP in apoptotic or unhealthy cells. By contrast, there was significant red fluorescence in the PEP-1-PRX2 sample similar to the control, although of a somewhat weaker intensity (Fig. 4C). This observation showed that PEP-1-PRX2 suppresses ROS-induced disruption of MMP.

On the basis of these observations, we measured the alteration of the levels of apoptosis markers such as Bax, cytochrome c, caspase 3, and poly ADP-ribose polymerase (PARP), in cells treated with PRX2 and PEP-1-PRX2. As shown in Fig. 5A, treatment with PEP-1-PRX2 significantly suppressed both the movement of Bax to mitochondria and the release of cytochrome c from mitochondria, while PRX2 failed to suppress them. In addition, cleavage of caspase 3 and PARP, increased by H_2O_2, was repressed by PEP-1-PRX2 (Fig. 5B). Furthermore, a TUNEL assay showed that DNA damage induced by H_2O_2 was significantly blocked by PEP-1-PRX2 in contrast with PRX2 and PEP-1 (Fig. 5C). Therefore, these results demonstrate that PEP-1-PRX2 could inhibit H_2O_2-induced activation of Akt, JNK, and p53, the disruption of MMP, and also the activation of intrinsic apoptosis pathway, subsequently resulting in protection of neuron cells from ROS.

3.5. Effect of PEP-1-PRX2 on survival of neurons and reactive gliosis in the hippocampal CA1 region

We investigated whether PEP-1-PRX2 has the capability to cross the BBB. PEP-1, PRX2, and PEP-1-PRX2 were i.p. injected in gerbils and gerbil brain homogenates were subjected to SDS-PAGE and Western blot analysis using an anti-His antibody. Western blot data showed that the injected PRX2 was not detected in the brain tissues of the PRX2-injected group (Fig. 6A and B), suggesting that the PRX2 failed to penetrate the BBB. However, in the brain tissues of the PEP-1-PRX2-injected group, there was a significant band, indicating that PEP-1-PRX2 protein traversed the BBB (Fig. 6B). Therefore, these results demonstrate that PEP-1-PRX2 could effectively cross the BBB of the gerbil, unlike PRX2 protein.

To assess the effect of PEP-1-PRX2 on ischemic damage-induced hyperactivity, spontaneous locomotor activity was observed before and after transient forebrain ischemic damage. The motor activities in the vehicle-, PEP-1-, and PRX2-treated groups were significantly increased at 1 day after ischemia/reperfusion, whereas PEP-1-PRX2 suppressed the increment of motor activity up to 60% of that in the vehicle-treated group (Fig. 7A).

Next we investigated whether PEP-1-PRX2 positively affects the survival of NeuN-immunoreactive neurons in the CA1 region against transient ischemic damage. As shown in Fig. 7B, in the PEP-1-PRX2 group, NeuN-immunoreactive neurons were abundantly detected in the stratum pyramidale (SP) of the CA1 region, like the control group, while, in PEP-1- and PRX2-treated groups, the numbers of NeuN-immunoreactive neurons were significantly decreased in the SP. To further examine the distribution of activated astrocytes and microglia in the CA1 region, the brain sections were stained with antibodies against GFAP, a marker of astrocytes, or Iba-1, a marker of activated microglia. In the case of astrocyte activation, the control group showed that GFAP-positive astrocytes had reduced cytoplasm with thin processes (Fig. 7C). Similarly, most GFAP-positive astrocytes found in PEP-1-PRX2-treated groups showed similar morphology to that in the control group and only a few astrocytes were activated (Fig. 7C). In contrast, in the vehicle-, PEP-1-, and PRX2-treated groups, GFAP-positive astrocytes were activated forms, characterized by punctuated cytoplasm with hypertrophied processes (Fig. 7C). Furthermore, Fig. 7D demonstrates that in the control group, Iba-1-immunoreactive

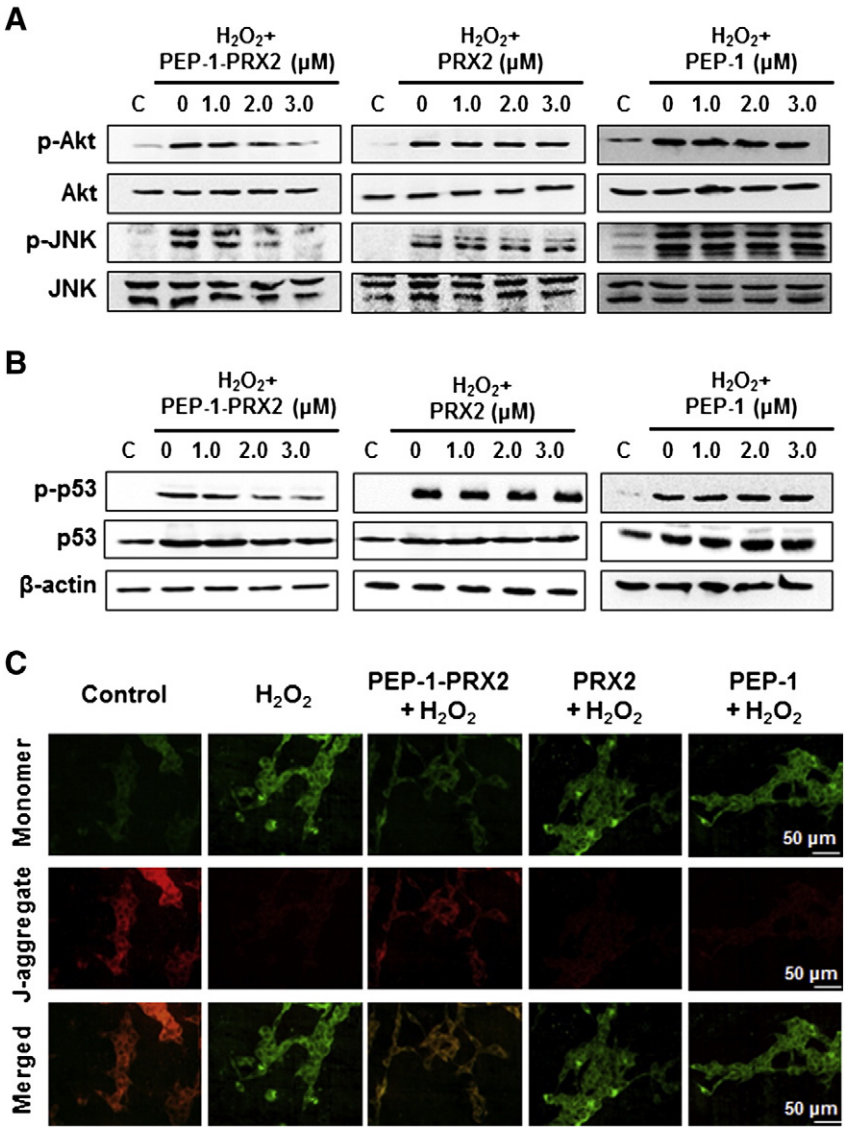

Fig. 4. PEP-1-PRX2 suppresses activation of Akt signaling and disruption of MMP in H_2O_2-treated HT22 cells. HT22 cells were pretreated with PEP-1, PEP-1-PRX2 and PRX2 (1.0–3.0 μM) for 1 h, washed with PBS, and then exposed to H_2O_2 (200 μM) for 15 min. The intracellular levels of Akt, JNK, and p53 were evaluated using Western blot analysis. (A) Inhibitory effect of PEP-1-PRX2 on H_2O_2-induced activation of PI3K/Akt and JNK. (B) Dose-dependent effect of PEP-1-PRX2 on phosphorylation of p53. C, untreated control cells. (C) Effect of PEP-1-PRX2 on H_2O_2-induced disruption of MMP. Changes of MMP were detected using JC-1 MMP assay kit. Control, untreated control cells. Red fluorescence, intact MMP; green fluorescence, loss of MMP.

microglia had round cytoplasm with thin long processes. On the other hand, in the vehicle-, PEP-, and PRX2-treated groups, Iba-1-positive microglia were significantly increased in the CA1 regions and especially exhibited the characteristic morphology of activated microglia, such as hypertrophied cytoplasm with retracted processes (Fig. 7D). By contrast, in the PEP-1-PRX2-treated group, Iba-1-positive microglia were mainly detected in the stratum oriens (SO) and stratum radiatum (SR), but rarely found in the SP.

3.6. Effects of PEP-1-PRX2 on lipid peroxidation in the hippocampus

4-HNE is highly formed during lipid peroxidation. 4-HNE protein conjugate levels in all groups were significantly increased 3 h after ischemia/reperfusion and thereafter the levels gradually decreased (Fig. 7E). As expected, 4-HNE levels in the PEP-1-PRX2 group were much lower than those in other groups. Therefore, these results showed that PEP-1-PRX2 prevented ROS generation resulting from ischemic damage and appreciably inhibited lipid peroxidation in the CA1 region.

4. Discussion

PRXs are widely expressed in mammalian tissues but, interestingly, the isozymes are differently distributed among different brain cell types [15]. PRX1 and PRX6 are localized in glial cells but not in neurons, whereas PRX2–5 proteins are widely detected in most neurons. However, PRX expression is low in dopaminergic neurons of the substantia nigra and in the CA1/2 pyramidal cells of the hippocampus [15]. The low expression of PRX2 is regarded as a potential cause of increased susceptibility to oxidative stress-induced diseases such as inflammation, Alzheimer's disease, and ischemic insults. Earlier studies have shown the neuroprotective roles of PRXs in oxidative stress-induced diseases. Intravenous injection of PRX3 decreased cerebral ischemic injury-induced lipid peroxidation, neuronal apoptosis, and activation of microglia and astrocytes [12]. Overexpression of PRX2 using an adenoviral vector protected cortical neuron cells from ischemic and oxidative damage [16]. MPP^+ treatment down-regulated the level of PRX2 in cultured cortical neurons but overexpression of PRX2 prevented the death of dopaminergic neurons in the SN in a MPTP-induced mouse model of Parkinson's disease [17]. Yao et al. observed

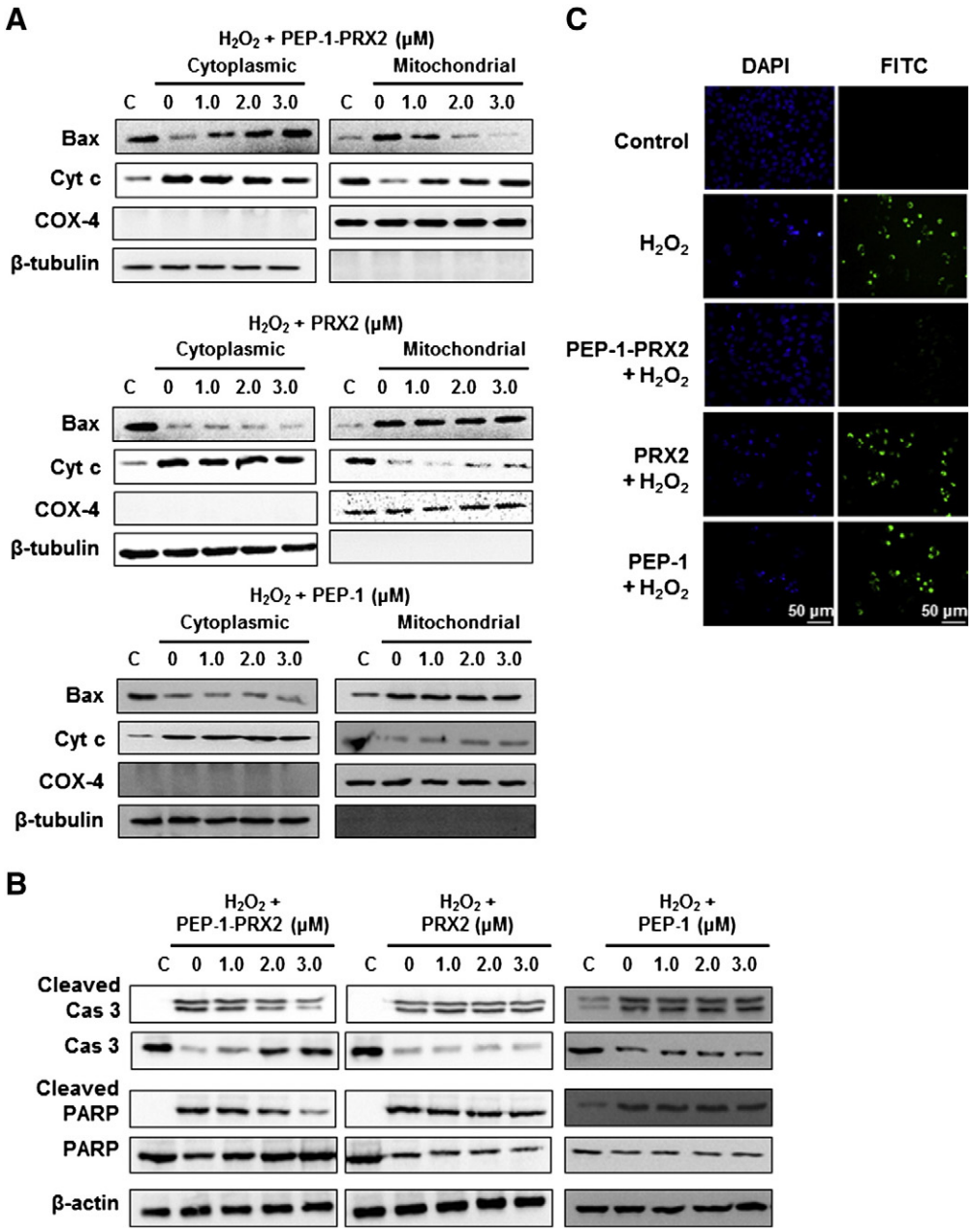

Fig. 5. PEP-1-PRX2 inhibits H_2O_2-induced intrinsic apoptosis activation and MMP dissipation. HT22 cells were pretreated with PEP-1-PRX2 and PRX2 (1.0–3.0 μM) for 1 h, washed with PBS, and then exposed to H_2O_2 (200 μM). Intact mitochondria and cytosol fraction were isolated using mitochondria isolation kit. The levels of Bax, cytochrome c, COX-4, a mitochondria marker, and β-tubulin, a cytosol marker, in each fraction were evaluated. (A) PEP-1-PRX2 inhibits cytochrome c release from mitochondria and insertion of Bax into mitochondria induced by H_2O_2. (B) PEP-1-PRX2 decreases the level of cleaved caspase-3 and PARP. C, untreated control cells. (C) Effect of PEP-1-PRX2 on H_2O_2-induced DNA fragmentation. HT22 cells were treated with PEP-1-PRX2, PRX2, and PEP-1 (3.0 μM) for 1 h and then with H_2O_2 (200 μM) for 10 h. TUNEL assay was performed to evaluate DNA damage.

that the increased expression level of PRX2 in Alzheimer's disease patients' brains provided protection for neurons against amyloid beta peptide induced toxicity [18]. In addition, it was reported that PRXs were involved in various cellular processes such as extension of life span, protection against excitotoxic stress, and tumorigenesis of astrocytic tumors [19–21]. Accordingly, the methods which enhance the levels of PRXs in various kinds of cells and tissues susceptible to oxidative stress may be effective in protecting those cells and tissues. Therefore, as shown in our previous studies [9,22,23], Figs. 2 and 6 also demonstrated that PEP-1-PRX2 could be used for the delivery of therapeutic molecules.

However, previous studies [14] reported that a mixing method, whereby proteins are mixed with CPP molecules, was as effective as the fusion method that we used in the present study. Furthermore, although our results (Fig. 2E) demonstrated that PRX2 can be transduced into HT22 cells by adding PEP-1-PRX2 fusion protein or PRX2 protein mixed with PEP-1 to the cells, the fusion method has potential advantage over the mixing method. With the mixing method, an excess of CPPs, a molecular ratio of 20:1, is required for multiple interactions with proteins and a maximal transduction of proteins into cells. In addition, proteins, when mixed with CPPs, can bind with an unequal number of CPPs, consequently producing proteins with different transduction efficiencies. Also, it seems feasible that uncombined CPPs alone can penetrate into target cells or tissues, which can negatively affect transduction efficiency of proteins or interrupt the transduction of proteins. On the other hand, with the fusion method, all CPP-fused proteins

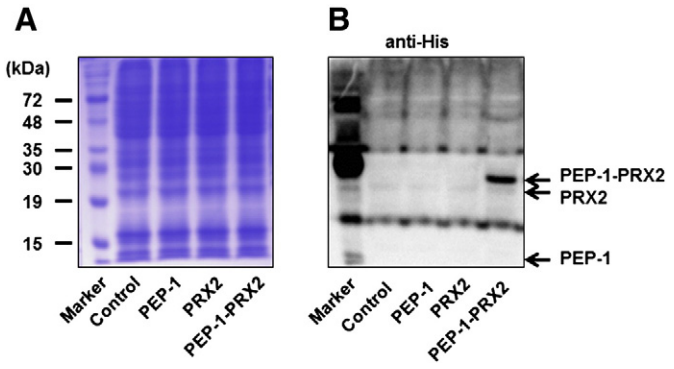

Fig. 6. *In vivo* transduction of PEP-1-PRX2 into brain tissues. PEP-1, PRX2, and PEP-1-PRX2 (3.0 mg/kg) were i.p. injected into gerbils 6 h prior to collection of gerbil brains. The levels of PEP-1, PRX2, and PEP-1-PRX2 in tissue homogenates were analyzed by (A) SDS-PAGE and (B) Western blotting using an anti-His antibody. The arrows indicate the approximate positions of PEP-1, PRX2, and PEP-1-PRX2.

have equal transduction efficiencies because the same number of CPP molecules is contained in each CPP-fused protein. Further, there are no unbound CPPs to disturb transduction. Therefore, for protein transduction into cells or tissues a fusion method may be considered more effective than a mixing method.

To understand the signaling pathway targeted by PEP-1-PRX2, we focused on whether PEP-1-PRX2 may affect activation of Akt, MAPK, and the apoptosis pathway triggered by H_2O_2. ROS are endogenously produced from cellular processes such as mitochondrial oxidative phosphorylation or in response to a variety of extracellular stimuli. It has been reported that ischemic injuries or ROS can activate pro-survival kinase signaling cascades such as PI3K/Akt and p42/p44 Erk1/2 through recruiting anti-apoptotic pathways [24] and also MAPK signaling pathways, including JNK, p38, and ERK, which, in turn, regulate gene transcription, the cell cycle, cellular differentiation, and cell death [25]. Notably, we confirmed that Akt, JNK, and p53 were activated less than 1 h after H_2O_2 treatment (Fig. 4). In contrast, we found that treatment with PEP-1-PRX2 suppressed the activation of Akt, JNK, and p53 in a dose-dependent manner (Fig. 4A and B). These results could be expected, given that PEP-1-PRX2 significantly suppresses the production of ROS in HT22 cells (Fig. 3B and C).

Apoptosis is a tightly regulated process including the loss of MMP, the activation of caspases, PARP cleavage, nuclear DNA fragmentation, and cellular shrinkage [26]. Activation of PI3K inhibits cell death by preventing both a translocation of Bax, the pro-apoptotic protein, to

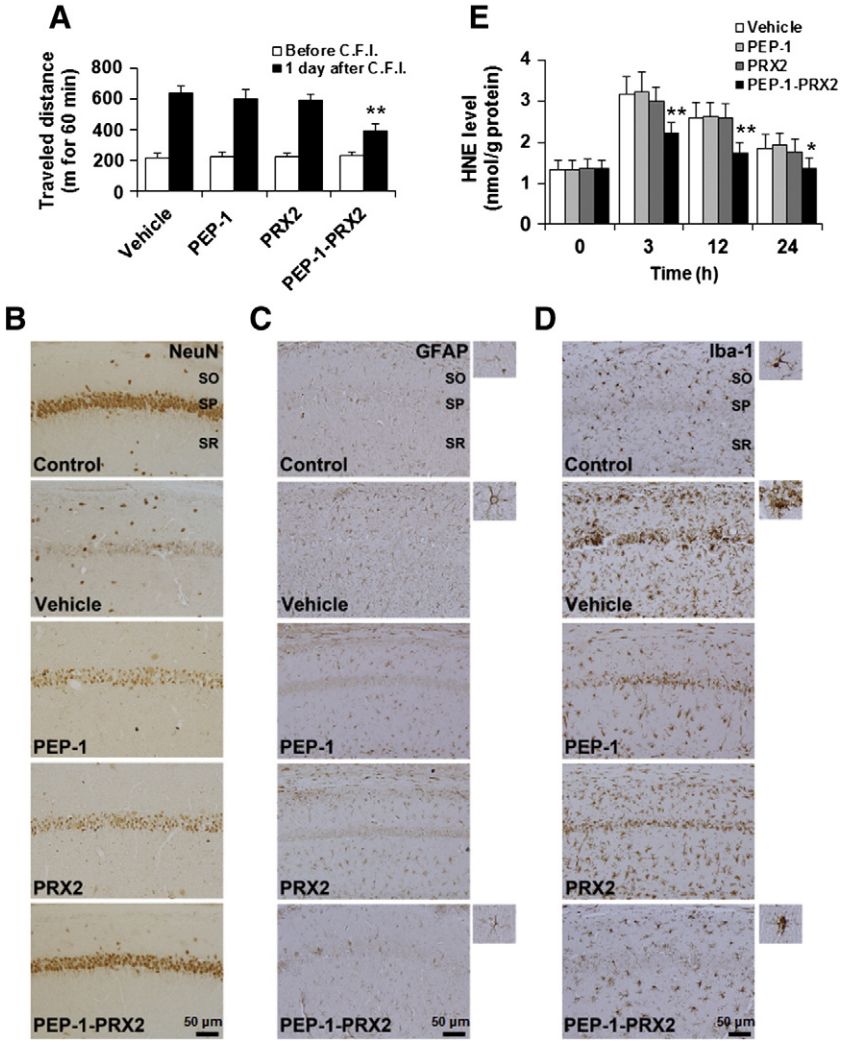

Fig. 7. PEP-1-PRX2 protects the CA1 region in the hippocampus against ischemic damage. (A) Effect of PEP-1-PRX2 on locomotor activity a day before and after ischemia/reperfusion. C.F.I., cerebral forebrain ischemic damage. Effect of PEP-1-PRX2 on the presence of (B) neurons, (C) astrocytes, and (D) microglia after ischemic insult. Brain sections were immunostained using a NeuN antibody against neurons, a GFAP antibody against astrocytes, and an Iba-1 antibody against microglia. SO, stratum oriens; SP, stratum pyramidale; SR, stratum radiatum. (E) Effect of PEP-1-PRX2 on lipid peroxidation in the hippocampus. The levels of 4-hydroxynonenal (4-HNE) protein conjugates in hippocampi were measured. The bar graph represents means ± SD. Data was analyzed by Student's *t* test.*$P < 0.05$ and **$P < 0.01$ between vehicle group and other groups.

the mitochondria and the formation of a pore in the outer mitochondrial membrane [24,27]. Thus, the opening of the mitochondrial permeability transition pore (mPTP) is known to occur under conditions of high calcium in the mitochondrial matrix. Consequently it leads to the passage of various molecules freely across the mitochondrial inner membrane, failure of ATP production, and irreversible damage to the cells [27]. As expected, we observed that PEP-1-PRX2 significantly prevented activation of Bax, the essential activator of mitochondrial dysfunction in cell death, release of cytochrome c from mitochondria, and activation of caspase-3, which leads to cleavage of PARP and fragmentation of DNA (Fig. 5). Based on our results, it appears that PEP-1-PRX2 protects HT22 cells against H_2O_2 through inhibiting the apoptosis pathway, including an opening of the mPTP, activation of Bax and caspases, and cleavage of PARP. Additionally, consistent with the above findings regarding the *in vitro* neuroprotective effect of PEP-1-PRX2, our studies significantly demonstrated that PEP-1-PRX2 protected the CA1 region in the hippocampus from ischemic reperfusion-induced oxidative damage and thereby inhibited the damage of motor function by ischemic reperfusion (Fig. 7A).

PRX isoenzymes are classified based on the mechanism and the number of cysteine (Cys) residues involved in the process of catalysis [3]. For example, PRX1-4 isozymes are homodimeric proteins that contain two conserved redox-active Cys residues at the N- and C-termini. The oligomeric properties of PRX2 were first reported to be promoted by various factors including ionic strength, pH, and the redox state of the active-site disulfide of PRXs. The Cys residues of PRXs are oxidized to sulfenic acid during reaction with oxidant substrates such as H_2O_2 and organic hydroperoxides [28]. The oxidation of Cys in PRXs leads to significant conformational changes and oligomerization [29]. Interestingly, it was found that the Cys residue at the active site of PRXs plays an important role in both cellular signaling and the removal of the oxidants because of the distinct relationship between the oligomeric state, redox status, and catalytic activity of PRXs [3]. For example, H_2O_2 produces toxicity in cells and tissues but, on the other hand, acts as a signaling molecule. For the role of H_2O_2 as a signaling molecule, it is necessary for H_2O_2 to evade PRXs and accumulate sufficient concentration in cells. PRX2 was inactivated through hyperoxidation of Cys at the active site [28,30], while PRX1 could be inactivated by a transient phosphorylation of Tyr-194 [30] or a hyperoxidation of Cys at its active site [28,30]. In addition, human PRX2 and yeast PRX1 and PRX2 were proposed to exert a chaperone-like function as well as a peroxidase function [7,31]. Thus, the presence and absence of the oxidant alter the extent of aggregation of PRX2 and the aggregated high molecular weight PRX2 functions as a chaperone protein [3,7,31]. Therefore, although many studies have increasingly revealed the recruitment of PRXs to the various cellular processes, it is necessary to more accurately understand the physiological functions beyond their catalysis activities.

In summary, PRXs are associated with oxidant defense and cellular redox regulation. PEP-1-PRX2 can have the ability to effectively transduce HT22 cells and brain tissues, and the transduced PEP-1-PRX2 can provide defense against oxidants through inhibiting ROS generation, apoptosis signaling, and cell death. In addition, we confirmed that, consistent with *in vitro* results, the transduced PEP-1-PRX2 exerts protection for the CA1 region of the brain in a transient ischemia–reperfusion model. Therefore, PEP-1-PRX2 may provide a new therapeutic approach against various oxidative stress-induced human diseases.

Acknowledgements

This work was supported by a Priority Research Centers Program grant (2009-0093812) and by a Basic Science Research Program grant (2012R1A1A2006995) through the National Research Foundation of Korea funded by the Ministry of Science, ICT & Future Planning of the Republic of Korea.

References

[1] H. Pradeep, J.B. Diya, S. Shashikumar, G.K. Rajanikant, Oxidative stress — assassin behind the ischemic stroke, Folia Neuropathol. 50 (2012) 219–230.
[2] M.V. Frantseva, P.L. Carlen, J.L. Perez Velazquez, Dynamics of intracellular calcium and free radical production during ischemia in pyramidal neurons, Free Radic. Biol. Med. 31 (2001) 1216–1227.
[3] L.B. Poole, A. Hall, K.J. Nelson, Overview of peroxiredoxins in oxidant defense and redox regulation, Curr. Protoc. Toxicol. S49 (2011) Chapter 7: Unit 7.9.
[4] S.W. Kang, H.Z. Chae, M.S. Seo, K. Kim, I.C. Baines, S.G. Rhee, Mammalian peroxiredoxin isoforms can reduce hydrogen peroxide generated in response to growth factors and tumor necrosis factor-alpha, J. Biol. Chem. 273 (1998) 6297–6302.
[5] M.H. Choi, I.K. Lee, G.W. Kim, B.U. Kim, Y.H. Han, D.Y. Yu, H.S. Park, K.Y. Kim, J.S. Lee, C. Choi, Y.S. Bae, B.I. Lee, S.G. Rhee, S.W. Kang, Regulation of PDGF signalling and vascular remodelling by peroxiredoxin II, Nature 435 (2005) 347–353.
[6] T.H. Lee, S.U. Kim, S.L. Yu, S.H. Kim, D.S. Park, H.B. Moon, S.H. Dho, K.S. Kwon, H.J. Kwon, Y.H. Han, S. Jeong, S.W. Kang, H.S. Shin, K.K. Lee, S.G. Rhee, D.Y. Yu, Peroxiredoxin II is essential for sustaining life span of erythrocytes in mice, Blood 101 (2003) 5033–5038.
[7] H.H. Jang, K.O. Lee, Y.H. Chi, B.G. Jung, S.K. Park, J.H. Park, J.R. Lee, S.S. Lee, J.C. Moon, J. W. Yun, Y.O. Choi, W.Y. Kim, J.S. Kang, G.W. Cheong, D.J. Yun, S.G. Rhee, M.J. Cho, S.Y. Lee, Two enzymes in one; two yeast peroxiredoxins display oxidative stress-dependent switching from a peroxidase to a molecular chaperone function, Cell 117 (2004) 625–635.
[8] W.S. Eum, D.W. Kim, I.K. Hwang, K.Y. Yoo, T.C. Kang, S.H. Jang, H.S. Choi, S.H. Choi, Y. H. Kim, S.Y. Kim, H.Y. Kwon, J.H. Kang, O.S. Kwon, S.W. Cho, K.S. Lee, J. Park, M.H. Won, S.Y. Choi, In vivo protein transduction: biologically active intact pep-1-superoxide dismutase fusion protein efficiently protects against ischemic insult, Free Radic. Biol. Med. 37 (2004) 1656–1669.
[9] D.S. Kim, E.J. Sohn, D.W. Kim, Y.N. Kim, S.A. Eom, G.H. Yoon, S.W. Cho, S.H. Lee, H.S. Hwang, Y.S. Cho, J. Park, W.S. Eum, S.Y. Choi, PEP-1-p18 prevents neuronal cell death by inhibiting oxidative stress and Bax expression, BMB Rep. 45 (2012) 532–537.
[10] E.J. Sohn, D.W. Kim, M.J. Kim, H.J. Jeong, M.J. Shin, E.H. Ahn, S.W. Kwon, Y.N. Kim, D.S. Kim, K.H. Han, J. Park, H.S. Hwang, W.S. Eum, S.Y. Choi, PEP-1–metallothionein-III protein ameliorates the oxidative stress-induced neuronal cell death and brain ischemic insults, Biochim. Biophys. Acta 1820 (2012) 1647–1655.
[11] P.X. Petit, H. Lecoeur, E. Zorn, C. Dauguet, B. Mignotte, M.L. Gougeon, Alterations in mitochondrial structure and function are early events of dexamethasone-induced thymocyte apoptosis, J. Cell Biol. 130 (1995) 157–167.
[12] I.K. Hwang, K.Y. Yoo, D.W. Kim, C.H. Lee, J.H. Choi, Y.G. Kwon, Y.M. Kim, S.Y. Choi, M. H. Won, Changes in the expression of mitochondrial peroxiredoxin and thioredoxin in neurons and glia and their protective effects in experimental cerebral ischemic damage, Free Radic. Biol. Med. 48 (2010) 1242–1251.
[13] M.S. Hershfield, L.J. Roberts 2nd, N.J. Ganson, S.J. Kelly, I. Santisteban, E. Scarlett, D. Jaggers, J.S. Sundy, Treating gout with pegloticase, a PEGylated urate oxidase, provides insight into the importance of uric acid as an antioxidant in vivo, Proc. Natl. Acad. Sci. U. S. A. 107 (2010) 14351–14356.
[14] M.C. Morris, J. Depollier, J. Mery, F. Heitz, G. Divita, A peptide carrier for the delivery of biologically active proteins into mammalian cells, Nat. Biotechnol. 19 (2001) 1173–1176.
[15] J. Goemaere, B. Knoops, Peroxiredoxin distribution in the mouse brain with emphasis on neuronal populations affected in neurodegenerative disorders, J. Comp. Neurol. 520 (2012) 258–280.
[16] S. Boulos, B.P. Meloni, P.G. Arthur, C. Bojarski, N.W. Knuckey, Peroxiredoxin 2 overexpression protects cortical neuronal cultures from ischemic and oxidative injury but not glutamate excitotoxicity, whereas Cu/Zn superoxide dismutase 1 overexpression protects only against oxidative injury, J. Neurosci. Res. 85 (2007) 3089–3097.
[17] D. Qu, J. Rashidian, M.P. Mount, H. Aleyasin, M. Parsanejad, A. Lira, E. Haque, Y. Zhang, S. Callaghan, M. Daigle, M.W. Rousseaux, R.S. Slack, P.R. Albert, I. Vincent, J. M. Woulfe, D.S. Park, Role of Cdk5-mediated phosphorylation of Prx2 in MPTP toxicity and Parkinson's disease, Neuron 55 (2007) 37–52.
[18] J. Yao, M. Taylor, F. Davey, Y. Ren, J. Aiton, P. Coote, F. Fang, J.X. Chen, S.D. Yan, F.J. Gunn-Moore, Interaction of amyloid binding alcohol dehydrogenase/Abeta mediates up-regulation of peroxiredoxin II in the brains of Alzheimer's disease patients and a transgenic Alzheimer's disease mouse model, Mol. Cell. Neurosci. 35 (2007) 377–382.
[19] S. Jarvela, I. Rantala, A. Rodriguez, H. Kallio, S. Parkkila, V.L. Kinnula, Y. Soini, H. Haapasalo, Specific expression profile and prognostic significance of peroxiredoxins in grade II–IV astrocytic brain tumors, BMC Cancer 10 (2010) 104.
[20] K.S. Lee, K. Iijima-Ando, K. Iijima, W.J. Lee, J.H. Lee, K. Yu, D.S. Lee, JNK/FOXO-mediated neuronal expression of fly homologue of peroxiredoxin II reduces oxidative stress and extends life span, J. Biol. Chem. 284 (2009) 29454–29461.
[21] F. Plaisant, A. Clippe, D. Vander Stricht, B. Knoops, P. Gressens, Recombinant peroxiredoxin 5 protects against excitotoxic brain lesions in newborn mice, Free Radic. Biol. Med. 34 (2003) 862–872.
[22] H.S. Choi, J.J. An, S.Y. Kim, S.H. Lee, D.W. Kim, K.Y. Yoo, M.H. Won, T.C. Kang, H.J. Kwon, J.H. Kang, S.W. Cho, O.S. Kwon, J. Park, W.S. Eum, S.Y. Choi, PEP-1–SOD fusion protein efficiently protects against paraquat-induced dopaminergic neuron damage in a Parkinson disease mouse model, Free Radic. Biol. Med. 41 (2006) 1058–1068.
[23] D.W. Kim, S.H. Lee, M.S. Jeong, E.J. Sohn, M.J. Kim, H.J. Jeong, J.J. An, S.H. Jang, M.H. Won, I.K. Hwang, S.W. Cho, T.C. Kang, K.S. Lee, J. Park, K.Y. Yoo, W.S. Eum, S.Y. Choi, Transduced Tat–SAG fusion protein protects against oxidative stress and brain ischemic insult, Free Radic. Biol. Med. 48 (2010) 969–977.

[24] D.J. Hausenloy, D.M. Yellon, New directions for protecting the heart against ischaemia–reperfusion injury: targeting the Reperfusion Injury Salvage Kinase (RISK)-pathway, Cardiovasc. Res. 61 (2004) 448–460.
[25] R.E. Burke, Inhibition of mitogen-activated protein kinase and stimulation of Akt kinase signaling pathways: two approaches with therapeutic potential in the treatment of neurodegenerative disease, Pharmacol. Ther. 114 (2007) 261–277.
[26] D.H. Lee, T. Park, H.W. Kim, Induction of apoptosis by disturbing mitochondrial-membrane potential and cleaving PARP in Jurkat T cells through treatment with acetoxyscirpenol mycotoxins, Biol. Pharm. Bull. 29 (2006) 648–654.
[27] S.A. Javadov, S. Clarke, M. Das, E.J. Griffiths, K.H. Lim, A.P. Halestrap, Ischaemic preconditioning inhibits opening of mitochondrial permeability transition pores in the reperfused rat heart, J. Physiol. 549 (2003) 513–524.
[28] Z.A. Wood, E. Schroder, J. Robin Harris, L.B. Poole, Structure, mechanism and regulation of peroxiredoxins, Trends Biochem. Sci. 28 (2003) 32–40.
[29] E. Schroder, J.A. Littlechild, A.A. Lebedev, N. Errington, A.A. Vagin, M.N. Isupov, Crystal structure of decameric 2-Cys peroxiredoxin from human erythrocytes at 1.7 Å resolution, Structure 8 (2000) 605–615.
[30] H.A. Woo, S.H. Yim, D.H. Shin, D. Kang, D.Y. Yu, S.G. Rhee, Inactivation of peroxiredoxin I by phosphorylation allows localized H_2O_2 accumulation for cell signaling, Cell 140 (2010) 517–528.
[31] J.C. Moon, Y.S. Hah, W.Y. Kim, B.G. Jung, H.H. Jang, J.R. Lee, S.Y. Kim, Y.M. Lee, M.G. Jeon, C.W. Kim, M.J. Cho, S.Y. Lee, Oxidative stress-dependent structural and functional switching of a human 2-Cys peroxiredoxin isotype II that enhances HeLa cell resistance to H_2O_2-induced cell death, J. Biol. Chem. 280 (2005) 28775–28784